Climate Services 30 (2023) 100380

Contents lists available at ScienceDirect

Climate Services

journal homepage: www.elsevier.com/locate/cliser

Evaluation of downscaling seasonal climate forecasts for crop yield forecasting in Zimbabwe

S. Chinyoka, G.J. Steeneveld *

Wageningen University, Meteorology and Air Quality Section, P.O. box 47, 6700 AA, Wageningen, The Netherlands

ARTICLE INFO

Keywords:
Seasonal forecasting
WRF
Crop
Zimbabwe
WOFOST
CFSv2

ABSTRACT

Meteorology and weather forecasting are crucial for water-limited agriculture. We evaluate the added value of downscaling seven-months global deterministic seasonal forecasts from the Climate Forecast System version 2 (CFSv2) using the Weather, Research and Forecasting (WRF) model over Zimbabwe for ten growing seasons (2011–2021). Downscaling reduces the area of significant differences between forecasted and observed total seasonal rainfall. Downscaling also improves the score for droughts as measured through the standardized precipitation index and 3-class method. Yield forecasts by the WOrld FOod STudies (WOFOST) model reveal that downscaling improves the estimated growing season evolution and maize yield in all studied regions across the country. For the main maize production region Karoi, the bias, root mean square error, mean absolute error and mean absolute percentage error reduce by 33% (0.2 ton/ha), 27% (0.4 ton/ha), 31% (0.4 ton/ha) and 27% (8.3 %) respectively by downscaling. Hence we illustrate that downscaling the deterministic seasonal forecasts may assist in food security in a crucial area in southern Africa.

Practical Implications

Climate, meteorology and weather forecasting are crucial for agriculture. Zimbabwe's climate has a high year-to-year variability of rainfall onset and amounts, leading to relatively large uncertainties for crop management, yield and farmer's income. In times of low domestic crop yield, the government will use crop yield forecasts to timely import food from the global market, which is thus crucial for decision making.

Our study illustrates how downscaling CFSv2 global seasonal forecasts (7 months ahead) over Zimbabwe using the WRF mesoscale meteorological model coupled to a crop yield forecast model can substantially reduce the error in estimated crop yield for the upcoming season. Downscaling enhances the spatial area of insignificant rainfall differences between model and observations in all OND, JFM and ONDJFM seasons, and thus substantially improves from coarse CFSv2 seasonal forecasts. Additionally, the success rate for the forecast standardised precipitation index improved from 60% to 73% in ONDJFM. Moreover, averaged over four test sites the root mean square error of the predicted maize yield reduces by 2.3 ton/ha (32%) due to the downscaling.

The results of our study implies that downscaled seasonal climate forecasts and crop forecast will be beneficial for decision making by local governments to secure food security. In particular the Southern African Regional Climate Outlook Forum (SARCOF, coordinated by the Southern African Development Community Drought Monitoring Centre) may benefit from this additional downscaled weather information in their seasonal forecasts (dry or wet season) three months prior to the rainfall season that they issue for farmers in the region. In addition, we recommend to make the developed procedure operational at national meteorological services.

* Corresponding author.
E-mail address: gert-jan.steeneveld@wur.nl (G.J. Steeneveld).

https://doi.org/10.1016/j.cliser.2023.100380

Available online 24 April 2023

1. Introduction

Agriculture heavily relies on weather and seasonal climate forecasts for water-limited food production (Ebhuoma, 2022). The Zimbabwean climate is characterised by a rainy season from mid-November until March, with a high spatiotemporal variability (Bhatasara, 2017; Mamombe et al., 2017), while the remaining months are dry (Bhatasara, 2017). Over the recent years, the increased frequency of dry spells lead to enlarged crop failure, particularly in January and February (Mamombe et al., 2017). The high crop failure is one of the factors reinforcing the high-level poverty in Zimbabwe, i.e. 63% of the population lives below poverty line. Also, agriculture is a relatively large economic sector that contributes for 15.5% to the Gross Domestic Product (period 1965–2018, Worldbank, 2021). The World Food Programme reported that almost 5.3 million Zimbabwean people are facing high risk of food insecurity (WFP, 2019). Climate variability and erratic rainfall are important drivers for this food insecurity in Zimbabwe (Bhatasara, 2017; WFP, 2019), and crop management relies on high quality seasonal weather forecasts (Phillips et al., 1998; Guido et al., 2020). Additionally, a recent study by (Chemura et al., 2022) projected a decline in maize production due climate change in Southern Africa including Zimbabwe. Seasonal rainfall forecasts are key for Zimbabwean agriculture, since 90% of smallholder farmers rely on rainfed agriculture (Bhatasara, 2017; Mushore, 2013; Unganai et al., 2013). Information about rainfall variability has been identified as one of the most useful pieces of information that subsistence farmers require in their preparations for planting. Therefore a research focus to better understand the physical controls of the rainfall variability was recommended (Tadross et al., 2005). However (Ebhuoma, 2022) highlighted that many stakeholders within Southern Africa fail to interpret and understand the seasonal climate forecasts in the form they are currently presented. This failure has reduced the uptake of seasonal climate forecasts leading to high maize crop failure hence the need to develop a complementary system. An increased demand for high-resolution seasonal climate forecasts at sufficient lead time emerged to allow response planning from users in agriculture, hydrology, disaster management, and health, among others (Kipkogei et al., 2017).

The movement and orientation of the intertropical convergence zone (ITCZ) largely influences the summer rainfall in Zimbabwe (Reason et al., 2006; Beilfuss et al., 2012), next to other mechanisms as the Tropical Temperate Troughs (Washington and Todd, 1999), cut-off lows originating from mid-latitude southern hemisphere weather systems (Favre et al., 2013), the Botswana upper air high (Unganai and Mason, 2002), and subtropical high-pressure systems. Moreover, El Nino (La Nina) is associated with dry (wet) summers in Zimbabwe (Mamombe et al., 2017). Also, Manjowe et al. (2018) found a considerable correlation between the Eastern Atlantic and the Western Indian Ocean sea surface temperatures (SSTs). The large-scale climate teleconnections patterns such as El Nino-Southern Oscillation (ENSO), Quasi-Biennial Oscillations and Indian Ocean Dipole and the slowly evolving southern hemisphere winter SST anomalies form the basis of statistical long-range rainfall forecasting methods (Mamombe et al., 2017; Unganai and Mason, 2002; Ismail, 1987; Makarau and Jury, 1997; Shukla, 1998; Koster et al., 2010).

Yearly, the Southern African Regional Climate Outlook Forum (SARCOF coordinated by the Southern African Development Community Drought Monitoring Centre) issues a binary ("dry" or "wet") seasonal rainfall forecast for mid-November to March based on these *statistical* forecasts (Mamombe et al., 2017; Unganai et al., 2013). However, (Kerandi et al., 2017) and (Nikulin et al., 2018) found that the *dynamical* downscaling of global seasonal forecasts improves the seasonal forecast reliability for East Africa, despite the performance differs regionally. Yuan et al. (2012) reported that downscaling CFSv1 using the Weather, Research and Forecasting model reduced the wet bias of seasonal mean rainfall by 25–71%. Furthermore, seasonal rainfall forecasts showed to have the potential to substantially improve crop yield forecasts at site and regional level in Burkina Faso (Mishra et al., 2008).

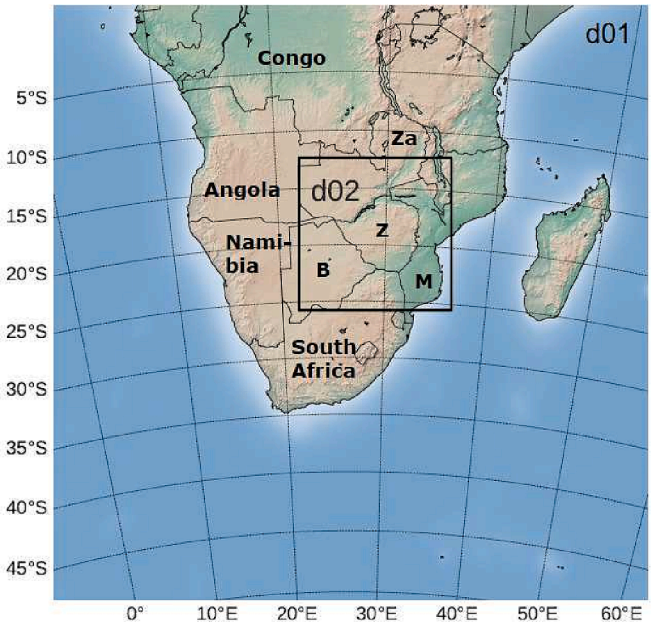

Fig. 1. Map of southern Africa, showing the position of Zimbabwe (Z), and its neighboring countries Botswana (B), Zambia (Za), and Mozambique (M). The borders of the map indicate the outer model domain used in WRF, while d02 indicates the nested domain.

Seasonal rainfall forecasts are only useful for farming systems if their accuracy is sufficient and spatially fine enough (Ziervogel et al., 2005). The current rainfall forecast accuracy within the SADC region (Fig. 1) is limited, especially for January-March (JFM) (Manatsa et al., 2011). Especially their spatiotemporal variability has a large room for improvement. More importantly, most African National Hydrological and Meteorological Services, including the Meteorological Services Department of Zimbabwe (MSDZ), do not produce seasonal weather forecasts operationally (Nikulin et al., 2018).

This study evaluates the downscaling of the global Climate Forecast System version 2 seasonal climate forecasts with the WRF mesoscale model, and quantifies the consequences of the downscaling for maize yield predictions in three regions in Zimbabwe using the WOFOST crop yield model (van Diepen et al., 1989; de Wit et al., 2019). New aspects in this study are the use of the CFSv2 model, which was not evaluated before for his region, and the use of the in situ and CHIRPS satellite precipitation observations, which is new with respect to earlier studies for this region. Finally, we assess the whole model chain containing CFSv2, WRF and WOFOST, and thus assess the complete time series of the modelled yield throughout the growing season, rather than the final yield only.

This paper has been organized as follows: Section 2 describes the materials and methods, Section 3 the results related to the meteorological modelling, Section 4 the results of the crop yield modelling, Section 5 the discussion and finally conclusions are drawn in Section 6.

2. Methods and Data

This section describes the models and meteorological observations used in this study.

2.1. Observations

This study uses two rainfall datasets. First, daily rain gauge observations from 35 MSDZ stations (see Appendix for locations) for 2011–2021 are used for model evaluation, i.e. whether the models

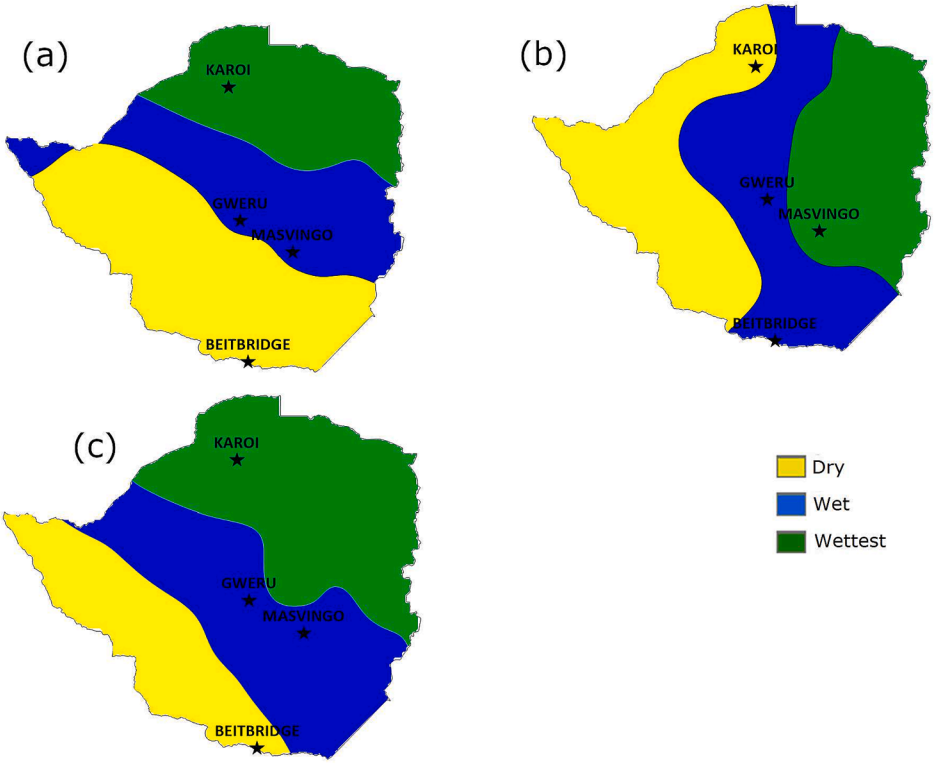

Fig. 2. Map of Zimbabwe indicating homogeneous rainfall zones for the period 1981–2019 for the seasons OND (a), JFM (b) and ONDJFM (c) with dry (yellow - labelled as region 1), wet (blue- labelled as region 2) and wettest (green - labelled as region 3). Study sites for crop yield are labeled Karoi, Gweru, Masvingo, and Beitbridge.

predict a normal or a relatively dry or wet crop seasons with respect to these observations. Also, we use the Climate Hazards Infrared Precipitation with Stations version 2 (CHIRPS, 4 km grid, daily frequency, Funk et al. (2015)) to overcome the limited surface data availability. CHIRPS data have two roles. First, they were used to calculate climatological rainfall means for 1981–2019, which act as reference to indicate whether the studied crop seasons were normal, or relatively dry or wet (see Section 2.5 below). Second, since annual rainfall differs strongly between the north and south of Zimbabwe, we stratify our model evaluation for three approximately homogeneous rainfall zones. CHIRPS data were used to determine these homogeneous rainfall zones (Section 3.1). Finally, we use soil water holding capacity information from World Soil Information for four crop sites (Beitbridge, Gweru, Masvingo, Karoi, Fig. 2).

2.2. ERA5

Since only rainfall observations were available to force the WOFOST crop model, daily ERA5 data on single levels (Hersbach et al., 2020) supplies solar radiation, 2-m air temperature and vapour pressure, and 10-m wind speed. Because local and regional records of actual yields are unavailable for 2011–2021, crop yields simulated using daily ERA5 data throughout the growing season are considered a proxy for the observed yields, and act as reference for evaluating the WRF- and CFSv2-based crop yields.

2.3. CFSv2

CFSv2 is a coupled atmosphere–ocean-land model for seasonal forecasts. It consists of four components, i.e. the Global Ocean Data Assimilation System (GODAS), National Center for Environmental Prediction (NCEP) Global Reanalysis, NCEP Global Forecast System and modular ocean model version 3 (Saha et al., 2014). CFSv2 has a spatial resolution of $\sim 100km$ and is used for operational forecasting up to 7 months ahead (Saha et al., 2014).

2.4. WRF

Our WRF model (Powers et al. (2017); Skamarock et al., 2019) applies the recommended setup of Kerandi et al. (2017), i.e. using the following physical parameterizations: Kain Fritsch Kain and Kain (2004) as cumulus scheme, WRF single-moment version 6 (WSM6) microphysics scheme (Hong et al., 2006), the Asymmetric Convective model version 2 Gilliam et al. (2007) for planetary boundary layer, the New Goddard scheme radiation scheme (Matsui et al., 2018) and the NOAH land-surface scheme (Kerandi et al., 2017; Pohl et al., 2011). We employ these schemes with an exception for the WRF single-moment version 7 microphysics scheme (Bae et al., 2019) with an additional representation for hail on top of WSM6. Forty vertical levels up to 20 hPa were used as in Kerandi et al. (2017).

We simulate ten rainfall seasons (October 1^{st}-March 31^{st}, for 2011–2021, since CFSv2 became operational in 2011) with spatial domains as in Fig. 1. The downscaling simulations receive boundary conditions every 6 h and were re-initialised every seven days to avoid model drift (Lo et al., 2008). In d01 (outer domain) and d02 (nested domain) the grid spacing amounts to 21 and 7 km, the domain size 280x280 and 215x215, time step 60 and 30 s and output saving interval 6 and 3 h respectively.

2.5. Rainfall season characterisation

To evaluate the models properly, we need to account for the large spatial difference in precipitation climatology across Zimbabwe. Therefore, Zimbabwe was divided into three homogeneous rainfall regions by Principal Component Analysis (Wilks, 2006) on CHIRPS rainfall data from 1981–2019. Fig. 2 shows three homogeneous regions within

Table 1
WOFOST model configurations at each site and growing degree days (GDD) from emergence to anthesis (TSUM1) and from anthesis to maturity (TSUM2). SWW denotes the soil moisture content at the wilting point, SMFCF the soil moisture content at field capacity, SM0 the soil moisture content at saturation, DEPTH the soil depth. Additionally *Zea mays L.* variety was used at all sites.

STATION	SWW (m3/m3)	SMFCF (m3/m3)	SM0 (m3/m3)	DEPTH (cm)	TSUM1 (GDD)	TSUM2 (GDD)
KAROI	0.10	0.237	0.337	159	825	600
GWERU	0.10	0.207	0.307	110	825	600
MASVINGO	0.10	0.216	0.316	200	825	600
BEITBRIDGE	0.10	0.263	0.363	200	825	600

Zimbabwe for seasons October-December (OND), JFM and October-March (ONDJFM). First, the seasonal rainfall forecast was evaluated using three categories, i.e. below normal (BN), near normal (NN) and above normal (AN). Seasonal rainfall below 75% of climatological mean falls under "below normal", between 75% and 125% are categorized as "near normal" and above 125% as "above normal" (Mushore, 2013). Second, we evaluate the seasonal drought forecast based on the standardized precipitation index (SPI) (Unganai et al., 2013; Keyantash, 2014; WMO, 1090).

$$SPI = \frac{x - \mu}{\sigma}. \tag{1}$$

with x the rainfall amount (mm), μ is the climatological mean rainfall (mm) from CHIRPS (see Section 2.1), and σ the climatological standard deviation which we evaluated for OND, JFM and ONDJFM. Here, a rainfall season was considered as a drought season (D) when the $SPI \leqslant -1$, a neutral season (N) when the $-1 < SPI < 1$, and a wet season (W) when $SPI > 1$ (Unganai et al., 2013).

2.6. Forecast evaluation

For model evaluation we use root mean square error (RMSE), mean bias error (MBE), mean absolute percent error (MAPE) and mean absolute error (MAE) as metrics (Willmott, 1982). The remapcon interpolation method (Schulzweida, 2014; Jones, 1999) from climate data operators was applied on CFSv2 and CHIRPS rainfall data to match the number of WRF grid cells (215*215) at 7 km grid spacing. We also report contingency tables for the SPI and 3-class rainfall forecasts (Stanski et al., 1989). Due to limited number of seasons available (CFSv2 was released in 2011), only proportion correct (PC) was used for model evaluation and assessing the added value of dynamical downscaling for rainfall.

2.7. Maize yield forecast

We use the WOFOST crop model which has been developed specifically for simulating crop yield in the tropics (van Diepen et al., 1989; de Wit et al., 2019). Within the model, the vegetation undergoes phenological stages from sowing to germination, flowering and yield production. WOFOST is widely used for wheat, maize, and sorghum with the ability to classify the output in terms of actual and potential production, and water or nutrient-limited production (de Wit et al., 2019). WOFOST has been calibrated, applied and validated for maize production in Kenya (Rötter, 1993); in the Central Rift Valley of Ethiopia (Kassie et al., 2014; Kassie et al., 2015); and in Tanzania in the Global Yield Gap Atlas project (van Ittersum et al., 2016). Although, actual maize yield values for Zimbabwe are scarce, we further evaluated the WOFOST model based on reported yields for the 1986–1987 and 1988–1989 crop seasons for Gweru and Harare sites respectively (see both Makadho, 1996). For Gweru the model forecasts 6.2 t/ha (4.9 assuming 20% reduction due to pests and diseases Savary et al., 2019) while 5.0 t/ha was observed. For Harare 8.0 t/ha (6.4 after reduction) was forecasted while 4.0 t/ha were observed.

Our downscaling study focuses on the weather variables from CFSv2 and WRF that are key to drive WOFOST:

- Daily maximum and minimum 2-m air temperature (°C)
- Daily rainfall (mm/day)

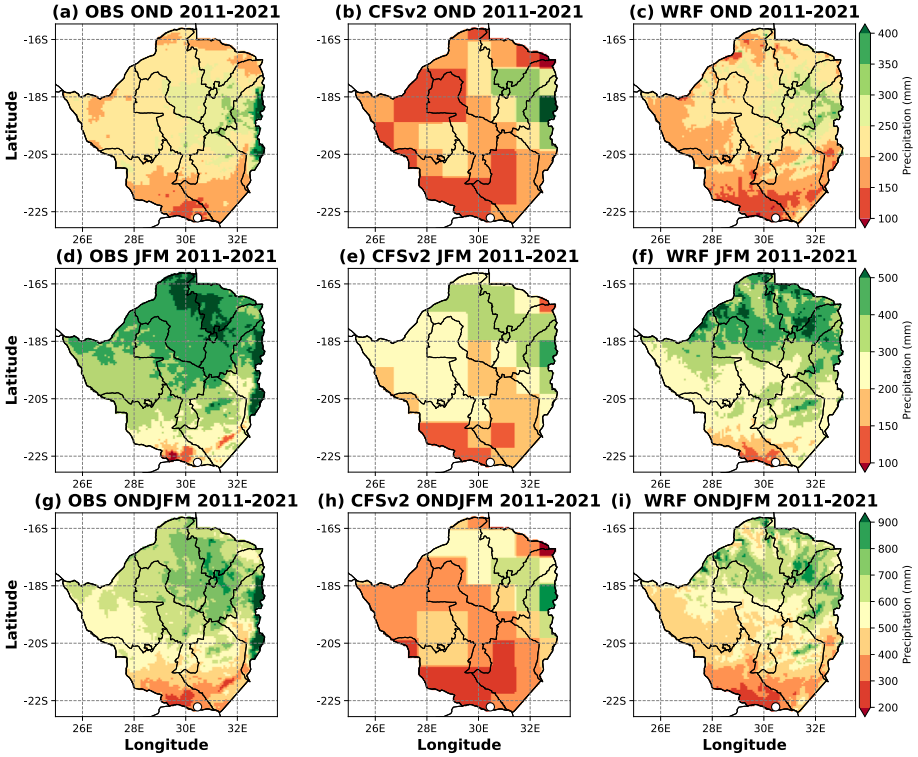

Fig. 3. Average modelled and observed (CHIRPS) seasonal rainfall for OND (a-c), JFM (d-f) and ONDJFM (g-i) for the period 2011–2021.

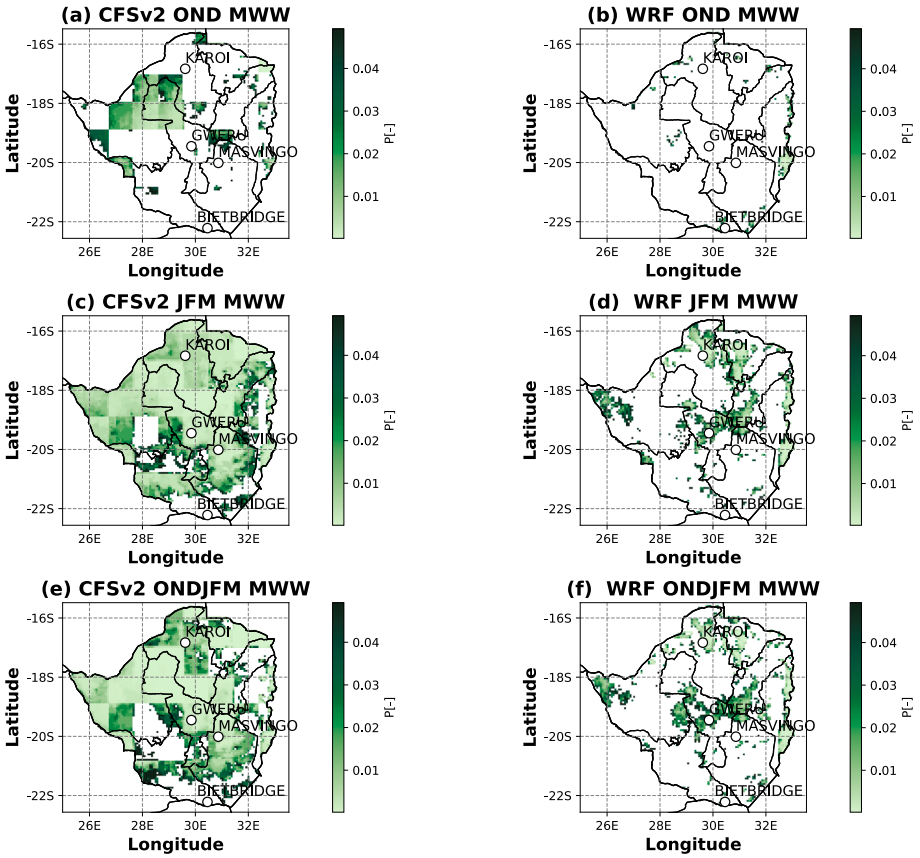

Fig. 4. Results of a Mann–Whitney U test metric of seasonal rainfall forecasts by WRF and CFSv2 for OND (a,b), JFM (c,d) and ONDJFM (e,f) for the seasons 2011–2021. The green shaded areas mark the region with a significant (5% level) difference between observed and modelled seasonal rainfall.

- Daily global radiation (J/m2/day)
- Daily mean 2-m wind speed (m/s)
- Daily mean 2-m vapor pressure (hPa)
- Onset and cessation of growing season dates generated from CFSv2 and WRF output

Finally, we configured WOFOST (Kassie et al., 2014) with *Zea mays L.* and with the soil characteristics and growing degree days as in Table 1. We performed water-limited production simulations factoring in water stress and assuming full control of pests, weeds and diseases. The simulated maize yields are evaluated where simulations forced by ERA5 data are used as proxies for observed maize yield. Our analysis focuses on four sites: Karoi (most maize production region), Gweru, Masvingo and Beitbridge (least maize producing region) (Phillips et al., 1998). Obviously, the onset of the rainfall season has huge impact on crop simulations. We determined the onset of rainfall season following (Odekunle, 2004) which sets the onset at the moment when 7–8% mean cumulative rainfall of the 5-day periods is attained. WOFOST model simulation end on March 31st, but the statistical model evaluation end at the moment in the season when the observed yield reaches a plateau.

3. Results: meteorology

This section reports about the model performances for the rainfall season.

3.1. Spatiotemporal rainfall distribution

The spatial distribution of total rainfall in ONDJFM ranges between 400–800 mm, 200–600 mm and 400–800 mm for observed (CHIRPS), CFSv2 and WRF respectively (Fig. 3g-i). The northern and eastern parts of Zimbabwe are wetter than the southern and western parts for OND (Fig. 3c) and and JFM (Fig. 3d-f) which in turn is also evident in the patterns for ONDJFM. This pattern is explained by the ITCZ positioning and the eastern highlands. The ITCZ has a larger influence over northern Zimbabwe while mountains in the east lead to orographically induced rainfall enhancement. Although both models capture the ITCZ influence, WRF has a better spatial coverage accuracy compared to CFSv2, especially for the western part of the country. However, overall WRF appears to be ∼100 mm too dry, while CFSv2 is ∼150 mm or more too dry. Despite both models underestimate the rainfall in OND, WRF outperforms CFSv2 (Fig. 3a-c).

Figs. 3a-f show that precipitation in JFM is largely influenced by the ITCZ which leads to high rainfall amounts over northern Zimbabwe, while in OND it is largely influenced by south-easterly winds fetching moisture from the Indian ocean. The relatively high WRF performance in OND, JFM and ONDJFM can be attributed to its ability to resolve local systems due to finer grid spacing. Considering that in the 2016–2017 and 2018–2019 seasons, the rainfall was characterised by tropical cyclones Dineo and Idai respectively, which are difficult to represent in seasonal forecasts, we find WRF performed reasonably well.

3.2. Mann-Witney U test of Seasonal rainfall forecasts

A Mann–Whitney U test (MWW) was conducted on the modelled seasonal rainfall forecasts and observations (Fig. 4). A testing at $\alpha = 0.05$ reveals a relatively high difference between CFSv2 seasonal forecasts and the observations, especially during JFM and ONDJFM. Importantly, the WRF forecasts appear to produce much larger areas without significant differences with observations. Only few regions showed significant differences between the model on one hand and observations on the other hand, as indicated by shaded regions in Fig. 4

Table 2
Modelled (WRF, CFSv2) and observed (35 surface station data) 3-class categories (AN = above normal, NN = near neutral, BN = below normal) of accumulated rainfall for ONDJFM (bold indicates model hit) for the three regions in Fig. 2c. The reference is the CHIRPS dataset for 1981–2019.

	3-CLASS								
ONDJFM	**REGION 1**			**REGION 2**			**REGION 3**		
SEASONS	**OBS**	**WRF**	**CFSv2**	**OBS**	**WRF**	**CFSv2**	**OBS**	**WRF**	**CFSv2**
2011–2012	NN	**NN**	AN	NN	**NN**	BN	NN	BN	BN
2012–2013	NN	**NN**	BN	NN	**NN**	**NN**	NN	**NN**	**NN**
2013–2014	AN	NN	BN	AN	NN	BN	NN	**NN**	BN
2014–2015	NN	BN	**NN**	NN	BN	BN	NN	**NN**	**NN**
2015–2016	NN	**NN**	BN	BN	**BN**	**BN**	BN	**BN**	**BN**
2016–2017	AN	NN	NN	AN	NN	NN	AN	NN	NN
2017–2018	NN	**NN**	**NN**	NN	**NN**	**NN**	NN	**NN**	**NN**
2018–2019	NN	BN	BN	NN	BN	BN	BN	**BN**	**BN**
2019–2020	NN	**NN**	BN	NN	**NN**	BN	BN	NN	**BN**
2020–2021	NN	**NN**	**NN**	NN	**NN**	BN	NN	**NN**	**NN**
PC		60%	30%		60%	30%		70%	70%

Table 3
Overview of proportion correct (PC) for the modelled accumulated rainfall by WRF and CFSv2 on the 3-class forecasts (AN, NN, BN) and SPI for the subseasons OND and JFM for the crop seasons in 2011–2020. Bold indicates best model.

	3-CLASS (%)				SPI(%)			
SEASON	OND		JFM		OND		JFM	
MODEL	WRF	CFSv2	WRF	CFSv2	WRF	CFSv2	WRF	CFSv2
REGION 1	**70**	50	**50**	20	**100**	80	**90**	50
REGION 2	**50**	30	**60**	40	**50**	30	**90**	40
REGION 3	40	**60**	**60**	30	40	**80**	**60**	50
NATIONAL	**53**	47	**57**	33	63	63	**80**	47

(b,c,f).

The MWW tests reveal that WRF fails to reproduce seasonal rainfall forecasts around the central watershed and mountainous regions i.e eastern Zimbabwe with altitude above 1.5 km, particularly in JFM. This may suggest the WRF model is unable to represent the orography sufficiently accurate at a grid spacing of 7 km.

3.3. Three-class seasonal rainfall forecasts with WRF and CFSv2

Seasonal rainfall forecasts from WRF and CFSv2 were compared with CHIRPS observations for all seasons and for homogeneous regions as determined by the PCA method (Fig. 2c). Table 2 shows the forecasted and observed precipitation category (near normal (NN), above normal (AN), below normal (BN) rainfall, with CHIRPS data from 1981–2019 as reference) for ONDJFM. WRF has more hits in ONDJFM compared to CFSv2. Apparently, downscaling of CFSv2 results improves the seasonal rainfall forecasts in OND as indicated by higher PC in two regions compared to CFSv2.

Our 3-class analysis for ONDJFM indicates that WRF results have an PC of 60%, 60% and 70 % compared to CFSv2 which has 30%, 30% and 70% for regions 1–3 respectively. Analyzing a complete season is important since the growing season stretches from October to March. Herein WRF outperformed CFSv2 in 3-class forecasting, which illustrates the added value of downscaling CFSv2. The impact of this slight increase is further tested using WOFOST below.

Table 3 summarizes the model results for the 3-class and SPI forecasts for the subseasons OND and JFM. When we focus on season OND, we find CFSv2 has a proportion correct of 50%, 30% and 60%, while WRF has a PC of 70, 50 and 40% for regions 1, 2 and 3 respectively (Table 3). Nationwide, WRF produces a PC of 53% while CFSv2 generates a PC of 47% which shows that WRF performed slightly better than CFSv2 in OND even though the PC is relatively low (bottom row in Table 3). Despite poor performances by both models in OND, WRF forecasts reduced the number of erroneous BN seasons in CFSv2 to NN,

Table 4
Modelled (WRF, CFSv2) and observed SPI categorization (W = wet, N = neutral, D = dry) for ONDJFM for the three regions in Fig. 2c. PC = proportion correct. Bold means a model hit.

	SPI category								
ONDJFM	**REGION 1**			**REGION 2**			**REGION 3**		
SEASONS	**OBS**	**WRF**	**CFSv2**	**OBS**	**WRF**	**CFSv2**	**OBS**	**WRF**	**CFSv2**
2011–2012	N	**N**	**N**	N	**N**	**N**	D	N	N
2012–2013	N	**N**	**N**	N	**N**	**N**	N	**N**	**N**
2013–2014	N	**N**	**N**	N	**N**	**N**	D	N	N
2014–2015	N	**N**	**N**	N	**N**	**N**	D	N	N
2015–2016	N	**N**	D	N	**N**	D	D	**D**	**D**
2016–2017	W	N	N	N	W	**N**	N	W	W
2017–2018	N	**N**	**N**	N	**N**	**N**	N	**N**	**N**
2018–2019	N	D	D	N	**N**	D	D	**D**	**D**
2019–2020	N	**N**	D	N	**N**	**N**	D	**D**	N
2020–2021	N	**N**	**N**	N	**N**	**N**	D	N	N
PC		80 %	60 %		90 %	80 %		50 %	40 %

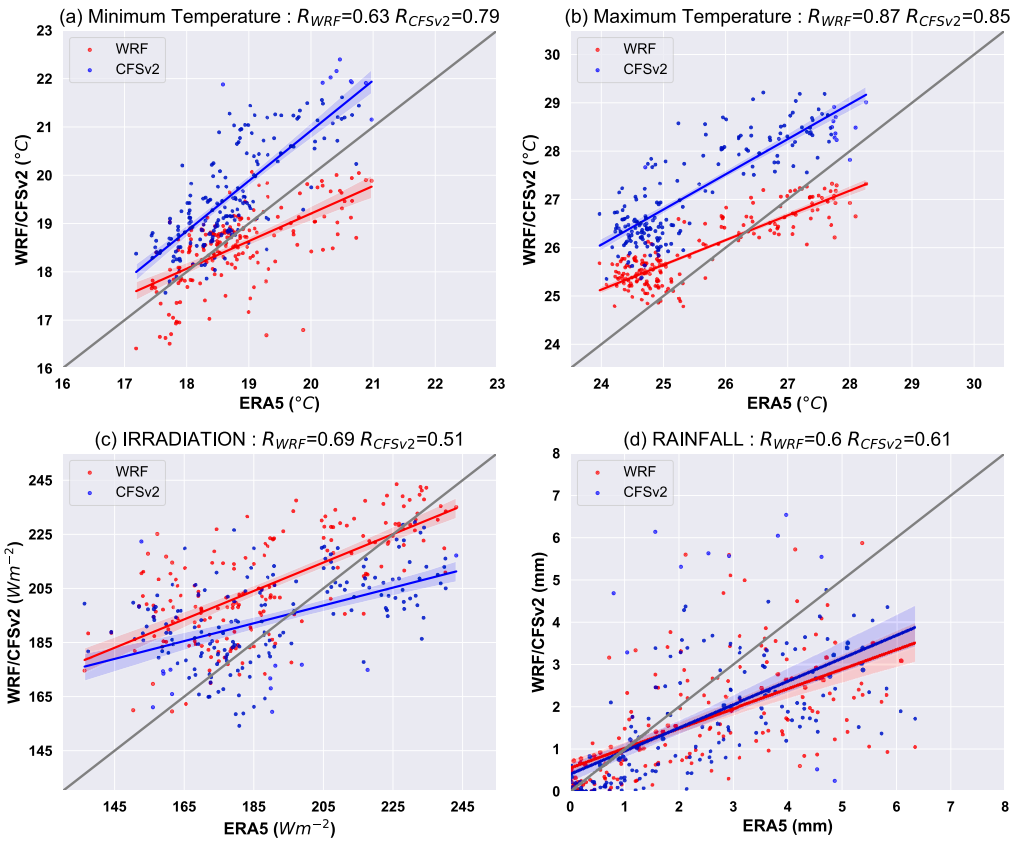

Fig. 5. Scatter plots of mean daily (a) T_{min}, (b) T_{max}, (c) irradiation (IRRAD), (d) rainfall (RAIN) in ERA5, CFSv2 and WRF for Karoi for 2011–2021 (n = 180), with correlation coefficient R (header). Red and blue shades mark the 90% confidence intervals.

which is a welcome improvement. Considering JFM, WRF performed fairly well in 3-class forecasting with a PC of 50%, 60% and 60% compared to CFSv2 with accuracy of 20, 40 and 30% for region 1, 2 and 3 respectively. The overall PC by WRF at national level is 57% while for CFSv2 is 33%. This result is consistent with findings in (Manatsa et al., 2011) who highlighted that rainfall forecasting is more skillful in the JFM season than in OND. This can be explained by the nature of the rain bringing systems. The ITCZ influence in JFM is highly predictable in most areas of the country compared to OND in which a number of systems are in play including westerly cloud bands known as Tropical Temperate Troughs.

3.4. SPI driven seasonal rainfall forecast

Categorisation of seasonal rainfall in terms of dry (D), wet (W) and neutral (N) indicated that WRF forecasted mostly neutral rainfall season while CFSv2 model has a bias towards dry conditions for ONDJFM (Table 4). More hits were achieved by WRF in all seasons compared to CFSv2. Considering the PC for ONDJFM, WRF appears outperforms CFSv2 in forecasting drought seasons. WRF results have a PC of 80%, 90% and 50% compared to 60, 80 and 40% in Region 1, 2 and 3 respectively. WRF forecasts more neutral (N) seasons in all seasons compared to CFSv2 which has bias towards dry (D) seasons.

Statistical evaluation of modelled SPI drought indices reveals that WRF outperforms CFSv2 in OND. WRF has an accuracy of 100%, 50% and 40%, for regions 1, 2 and 3 respectively (Table 3), while CFSv2 has an accuracy of 80%, 30% and 80% in OND for region 1, 2 and 3 respectively (Table 3). Downscaling appears to improve the performance in JFM with an accuracy of 90%, 90% and 60% against CFSv2 scores of 50%, 40% and 50% for region 1, 2 and 3 respectively. The nationwide model performance for JFM amounts to 80% for WRF and 47% for CFSv2 for the SPI (Table 3). Moreover its is interesting to note

Table 5
Correlation coefficients between WRF, CFSv2 and ERA5 for the modelled screen level T_{min}, T_{max}, vapour pressure, wind speed, surface irradiation, best scores in bold.

Site	ERA5 vs	T_{min}	T_{max}	Wind speed (2 m)	Irradiation	Vapor pr.
Karoi	WRF	0.63	**0.87**	0.73	**0.69**	0.93
	CFSv2	**0.79**	0.85	**0.79**	0.51	0.93
Gweru	WRF	**0.61**	**0.56**	0.09	**0.38**	0.83
	CFSv2	0.61	0.50	0.09	0.29	**0.86**
Masvingo	WRF	**0.59**	**0.60**	0.057	**0.33**	0.82
	CFSv2	0.43	0.29	**0.29**	0.36	**0.86**
Beitbridge	WRF	**0.72**	**0.16**	0.17	**0.2**	0.80
	CFSv2	0.48	0.07	**0.31**	0.15	**0.85**

that the anomaly correlation coefficient (ACC), which is an indicator for the model representation of the year-to-year variability increased from 0.023 (CFSv2) to 0.62 (WRF) in region 1, from 0.06 (CFSv2) to 0.72 (WRF) in region 2, but decreased from 0.75 (CFSv2) to 0.53 (WRF). These values indicate that in region 3 an improved rainfall climatology dominates the enhanced scores through downscaling, while in regions 1 and 2 also the year-to-year variability was better captured. However, the sample size of 10 years is relatively short for the ACC analysis.

3.5. Evaluation of weather variables for maize yield forecast

Modelled key weather variables for crop modelling (2-m minimum and maximum air temperature (T_{min},T_{max}), 2-m wind speed, surface solar irradiation, 2-m vapor pressure) were evaluated against ERA5 and correlation coefficients (r) are estimated. Fig. 5 and Table 5 show a strong positive correlation between modelled T_{max} and ERA5, with WRF having a slightly higher correlation compared to CFSv2 at Karoi. Also,

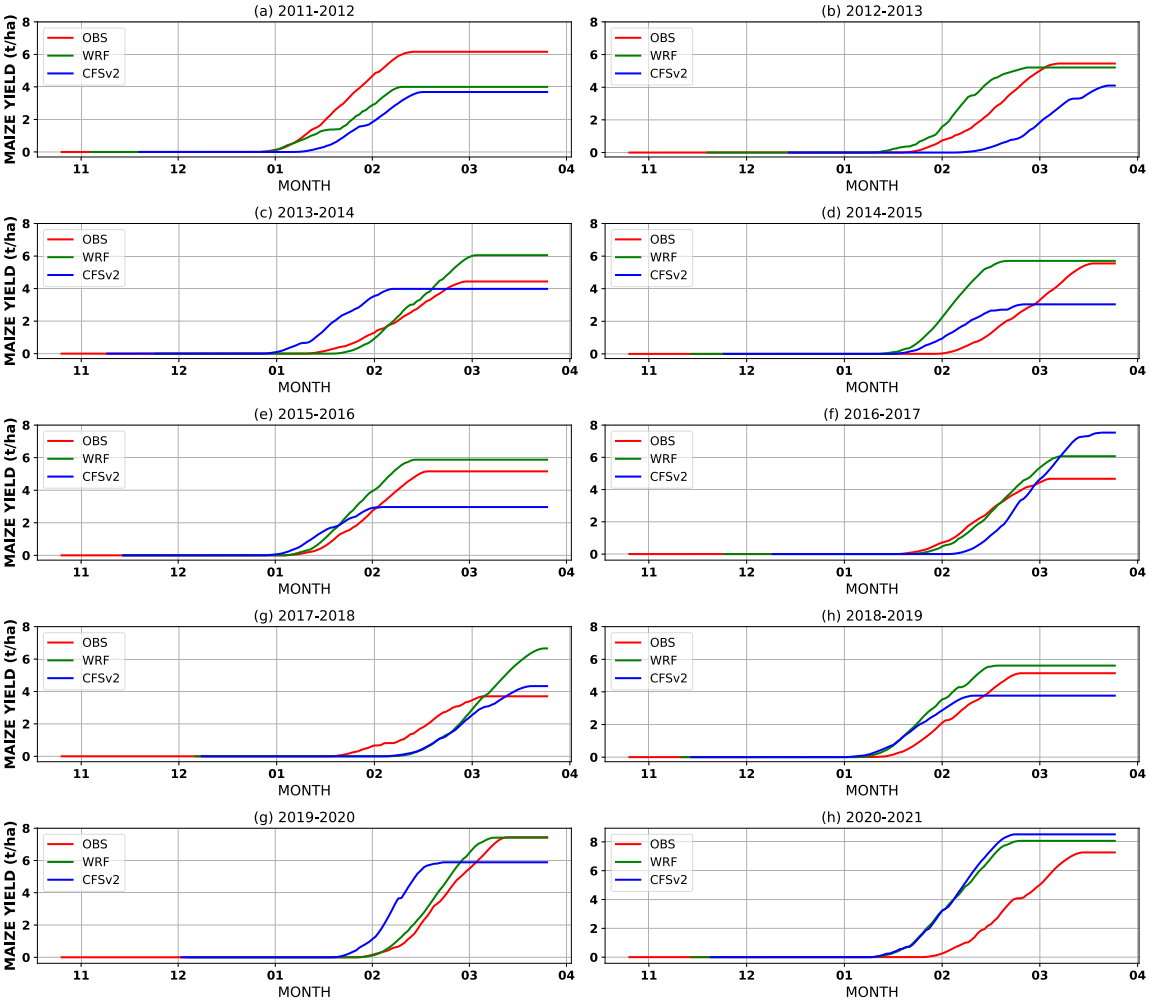

Fig. 6. Times series of simulated maize yield at Karoi using WRF-WOFOST, CFSv2-WOFOST and ERA5-WOFOST (OBS) weather data for the 2011–2021 rainfall seasons.

both T_{min} and T_{max} are closer to the 1:1 line in WRF than in CFSv2. The latter produces a warm bias of 1 K and 1.5 K for T_{min} and T_{max} respectively. With this warm bias the required TSUM to anthesis and to maturity (Table 1) will be reached earlier in time, will be discussed later on in more detail. Further analysis for T_{min}, vapour pressure and irradiation suggests that both WRF and CFSv2 represent clouds differently even though they have the same correlation coefficient for rainfall (r = 0.6). Model results for irradiation suggest that WRF produces less clouds than CFSv2 over Karoi. WRF forecasts have a moderate correlation (r = 0.69) with the observed irradiation which also translated into stronger relationship in T_{max}. This can be explained by the effect of clouds on incoming shortwave radiation which is a main contributor in daily T_{max}. Also, the smaller cloud cover in WRF leads to lower T_{min}. Moreover, higher wind speed influences the turbulent intensity which in turn limits the surface cooling. This can be confirmed by moderate correlation for wind speed leading to a moderate correlation with T_{min} by WRF forecasts, while CFSv2 forecasts have a high correlation between wind speed and T_{min}. We find poorer scores for Gweru, Masvingo and Beitbridge, particularly for wind speed and irradiation (Table 5). Typically WRF outperforms CFSv2 in irradiation, T_{min} and T_{max}, and CFSv2 performs slightly better for 2-m wind speed and vapour pressure (Table 5).

4. Results: Maize yield forecasting using WOFOST

This section assesses the impact of downscaling on the WOFOST crop yield forecasts for the four sites. As expected the highest yield is reached for Karoi, and the smallest for Beitbridge. Averaged over the ten seasons 4.4 t/ha/y maize production has been modelled in Karoi, while for Beitbridge only 2.0 t/ha/y of maize production is found. We present the simulated evolution of the maize yield at Karoi (Fig. 6) for the ten selected cropping seasons to demonstrate the effect of onset and cessation of a farming season. We further quantify the absolute yield differences between simulations forced by ERA5, WRF and CFSv2 for *Zea mays L.* (ERA5-WOFOST, WRF-WOFOST and CFSv2-WOFOST respectively). Subsequently we evaluate the WOFOST model simulations not only on the final yield, but also on the yield evolution in time.

4.1. Karoi

Concerning the simulated maize yield we find that WRF-WOFOST outperforms CFSv2-WOFOST for Karoi (Fig. 6), since in seven of the ten simulated seasons the final yield by WRF-WOFOST is closer to the observations than CFSv2-WOFOST. Furthermore, it is interesting to note that the warm bias in CFSv2 results in a relatively early grain setting more often in CFSv2-WOFOST (6 times earlier than observed) than in WRF-WOFOST (4 times earlier than observed). The warm bias promotes an earlier completion of the required temperature sum for the phenological stages, therefore a faster grain settting. In seasons 2011–2012, 2015–2016 and 2018–2019 the modelled and observed time of grain set is approximately correct, while in other seasons the models deviates

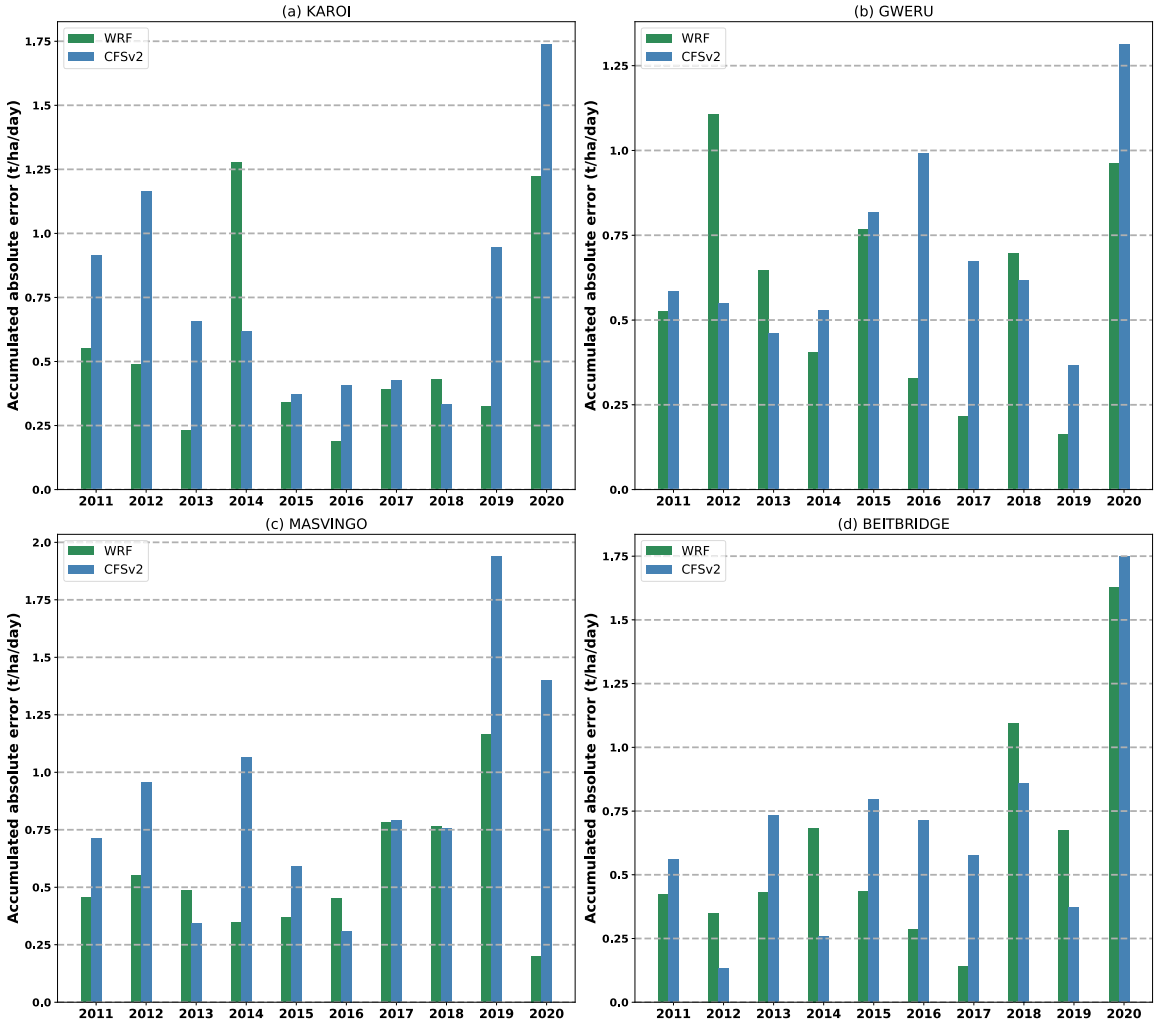

Fig. 7. Maize yield accumulated absolute error for WRF-WOFOST and CFSv2-WOFOST for (a) Karoi, (b) Gweru, (c) Masvingo, (d) Beitbridge for 2011–2020 rainfall seasons. The accumulated error is calculated till the observations reach a yield plateau in Fig. 6.

from the observations. E.g. in 2012–2013 and 2016–2017 the grain setting in CFSv2-WOFOST is too late, while in 2013–2014 and 2019–2020 it is substantially too early in CFSv2. In 2013–2014, both OND and JFM were too dry in CFSv2 (SPI metric, not shown), with underestimated cloud cover and overestimated temperatures, which promote early grain setting, but results in a low yield due to drought stress in JFM. In 2014–2015 both models were too dry in JFM which explains the different yield evolution than observed. In 2015–2016 CFSv2 generated a too dry JFM which is expressed in a lower final yield than observed. WRF-WOFOST slightly delays the grain setting in 2014–2015. In 2016–2017 the underestimated final yield by WRF-WOFOST can be explained by the fact that the WRF model generated a neutral SPI, while in reality a relatively wet season was observed and modelled in CFSv2 (not shown). WRF-WOFOST outperforms CFSv2-WOFOST in almost all seasons particularly in 2013–2014, 2015–2016 and 2016–2017 seasons where WRF-WOFOST accurately predicted the onset of grain setting. The average simulated maize yield for Karoi amount to 4.4 t/ha, 4.8 t/ha and 3.8 t/ha for ERA-WOFOST, WRF-WOFOST and CFSv2-WOFOST respectively.

In addition, we evaluate the model performance by taking in integrated error metric over the season by accumulating the absolute error between model and observations over time in Fig. 6 until the observations reach a yield plateau, and divide by the simulation time to express the error in t/ha/day. In this way the model simulations are not only penalized for a bias in final yield, but also for a biased evolution in the growing season. As such biases in the temperature sum that governs the forecasted plant phenology and precipitation biases that affect the yield are acknowledged. Fig. 7a shows that WRF-WOFOST performed better than CFSv2-WOFOST in eight of the ten seasons. In 2011–2012, 2012–2013 and 2016–2017 CFSv2 has a relatively large error due to a delayed onset of the yield, while in seasons 2013–2014 and 2019–2020 CFSv2 is too early. During the 2014–2015 season, the WRF-WOFOST and ERA5-WOFOST simulation have almost similar maize yield at maturity however the accumulated error for WRF-WOFOST is relatively high due to differences in rainfall distribution. WRF-WOFOST even performed poorly compared to CFSv2-WOFOST during that season.

4.2. Gweru

Maize yield simulations (Fig. 7b) show relatively poor results for both models, which is consistent with the relatively weak correlation between observed and modelled weather variables, particularly for irradiation, minimum and maximum temperatures (Table 5). Nevertheless, WRF-WOFOST performed better than CFSv2-WOFOST in seven seasons considering the accumulated absolute crop yield error. The average maize yields at Gweru amount to approximately 4.2 t/ha, 4.3 t/ha and 3.4 t/ha for ERA5-WOFOST, WRF-WOFOST and CFSv2-WOFOST respectively. A decline in correlation of modelled and observed weather

Table 6
Error statistics of WRF-WOFOST and CFSv2-WOFOST and ERA5-WOFOST (reference) maize yield predictions. Bold: best scores.

	KAROI		GWERU		MASVINGO		BEITBRIDGE	
SCORE	**WRF**	**CFSv2**	**WRF**	**CFSv2**	**WRF**	**CFSv2**	**WRF**	**CFSv2**
MBE (t/ha)	**0.4**	−0.6	**0.1**	−0.8	**−0.3**	−2.0	0.3	**0.2**
RMSE (t/ha)	**1.1**	1.5	1.6	**1.4**	**1.1**	3.0	**1.1**	1.3
MAE (t/ha)	**0.9**	1.3	1.4	**1.3**	**0.9**	2.3	1	1
MAPE (%)	**22.4**	30.7	35.1	**29.8**	**26**	49.5	**107**	133

variables at Gweru (region 2) compared to Karoi (region 3) suggests that seasonal forecasts are more promising in the latter region.

4.3. Masvingo

Fig. 7c show the results of accumulated absolute maize error for Masvingo. Analysis of weather data for the Masvingo site showed weak correlations of maximum and minimum temperature, irradiation and a high correlations on water vapour (Table 5). The weak correlations on irradiation, temperatures and rainfall plays a key role in crop simulations for both models. CFSv2 forecasts have a better rainfall correlation than WRF forecasts. However, WRF-WOFOST outperforms CFSv2-WOFOST, and findings are consistent with findings for Gweru, which underlines the robustness of our results. The average maize yield at Masvingo amounts to 4.2, 4 and 2.2 t/ha for ERA5-WOFOST, WRF-WOFOST and CFSv2-WOFOST respectively.

4.4. Beitbridge

A moderate relation between minimum temperatures for both models at the Beitbridge site was observed (Table 5). All other weather parameters showed negligible relations except for vapour pressure which at all sites showed strong relation. Comparing the strength of the relation of rainfall for both models indicate that CFSv2 results have a better correlation than WRF results for which even both relations are too weak. This again suggests that CFSv2 weather data as better chances of performing better in maize yield simulations at this site. The maize yields simulations forced by CFSv2 and WRF weather data are poor over 2011–2012, 2012–2013 and 2015–2016 seasons. The average ERA5-WOFOST, WRF-WOFOST and CFSv2-WOFOST maize yields amount to 2.0, 2.3 and 2.2 t/ha respectively.

Summarizing the results we find that the regions with relatively poor seasonal forecasts such as Beitbridge, Gweru and Masvingo are categorised by poor maize yields due to relatively limited predictability of rainfall. The performance of WRF in forecasting seasonal rainfall and maize yield decreased as we move from region 3 to region 1. Statistical analysis of the maize yield simulations from WRF and CFSv2 is outlined in Table 6. The MAPE for WRF-forced forecasts is 22.4% while CFSv2 has a MAPE of 30.7% for Karoi. In addition, the ACC for the forecast maize yields decreased from 0.38 to 0.29 for Karoi, while for Gweru ACC changed from 0.31 to 0.39, for Masvingo from −0.22 to 0.79 and for Beitbridge from 0.42 to 0.64. This indicates that particularly also the year-to-year variability representation improved for the latter three stations. Evaluating using all the metrics shows that yield forecasts driven by WRF outperform forecasts driven by CFSv2 at Karoi. The accuracy of maize yield forecasts decreases substantial in Gweru, Masvingo and Beitbridge sites as indicated by poor correlation of other weather parameters.

The evaluation of maize yield prediction indicated that WRF-WOFOST yields performed reasonably in the northerly region 3, represented by Karoi, with a MAPE of 22.4%, bias of 0.4 t/ha when evaluated against ERA5-WOFOST. A bias reduction from −0.6 to 0.4 t/ha and MAPE reduction from 30.7% to 22.4% in region 3 is a substantial improvement achieved through downscaling. Also, WRF-WOFOST simulations outperformed CFSv2-WOFOST in Karoi and Masvingo in all metrics (Table 6).

5. Discussion

5.1. WRF performance

The accuracy of current routine statistical seasonal forecasting by SARCOF in Zimbabwe amounts to 40–65% in OND and 50–70% in JFM (Manatsa et al., 2011). Dynamical downscaling of CFSv2 using WRF in our study has the accuracy of 53% in OND and 57% in JFM. Moreover, downscaling also represents a better spatial variation that can be beneficial for stakeholders in agriculture. Despite the relatively small sample size of 10 seasons, our results are encouraging. Further evaluation is encouraged in the future, especially since forecasting a season influenced by tropical cyclones 7 months in advance is challenging. The effect of such anomalies can be evened out if the number of seasons could be increased.

In addition to the effects of downscaling, crop yield forecasts may benefit from ensemble forecasting of the meteorological fields, in order to quantify the model uncertainty (see e.g. Ogutu et al., 2018 who downscaled SYSTEM4 ensemble forecasts from about 80 km to 50 km). However, CFSv2 does only offer one simulation every six hours (00, 06, 12, 18 UTC), and evaluating the downscaling of these members at 7 km grid spacing would be computationally too expensive on the one hand, and mix effects of varying starting times and downscaling on the other hand, which we aim to avoid. However, the improvements seen through downscaling here through better representation of the orography and the atmospheric physical processes suggest downscaling will be beneficial for other members as well.

Also, our statistical estimates between model and CHIRPS rainfall data were based on regridded rainfall data. The interpolation introduced an error which is estimated to be maximum 0.4% (Jones, 1999), and is as such not expected to affect our conclusions.

The selected physical parameterizations are important for forecasting rainfall and near surface meteorology. Crétat et al. (2012) concluded that rainfall amounts and their geography, intensity, and intraseasonal characteristics are predominantly sensitive to convection schemes, and less to boundary-layer and microphysics schemes. They found Kain-Fritsch to produce wet rainfall amount biases, in contrast to our study. Also, the Yonsei University (YSU) planetary-boundary layer (PBL) scheme produces systematically wetter rainfall biases in South Africa than when combined with the Asymmetrical Convective Model-version 2 model (ACM2).

Interestingly, Robertson et al. (2012) evaluated downscaling techniques for seasonal rainfall forecasts from GCMs and RCMs over the Philippines, and showed that spatial interpolation and model output statistics (MOS) do have their value. At the station scale the ACC of the spatially interpolated RCM data outperformed the spatially interpolated GCM data for seasonal rainfall. MOS results appeared to be quickly superior, both for GCM and RCM data. However, MOS results appeared region-depended and sensitive to the length of the training dataset.

Ratnam et al. (2013) used WRF to downscale 3-month seasonal forecasts by the global SINTEX–Frontier Research Center for Global Change model for Southern Africa. Substantial improvement in the spatial rainfall distribution after downscaling was found, but also a higher positive rainfall bias with a prescribed SST, compared to a time-evolving SST through an ocean mixed-layer model. This was mainly due to improved surface fluxes over the Indian Ocean, and subsequent

evolution of weather patterns to the inland of southern Africa. Future downscaling should take this dynamic SST evolution into account.

de Lange et al. (2021) evaluated several PBL schemes for multiple sites in Southern African Highfield. For June the Mellor–Yamada–Nakanishi–Niino scheme appeared the best performing scheme for temperature, while other schemes like ACM2 are close to the best score. For November the Mellor-Yamada-Janjic scheme outperformed the other schemes. The ACM2 scheme as used in our study performed worse for RH but best for the PBL height. Note that evaluation results differ per region. In addition, South Africa is more affected by mid-latitude weather than tropical weather than Zimbabwe, which hampers a one to one comparison to our study.

Moreover, Somses et al. (2020) evaluated WRF for an extreme precipitation event in southern Africa, with the focus on Namibia. The impact of nesting was found to be small. Switching off the convection schemes resulted in high rainfall intensity and increased detail in the simulations, even for a grid spacing of 9 km. Using a grid spacing of 3 km and an activated convection scheme, results in a loss of detail in the simulations as well as lower rainfall amounts. With a grid spacing of 7 km and convection scheme on, our selected model setup is beneficial concerning both aspects.

Related to hurricane impacts, Bopape et al. (2021) evaluated WRF multiple convection schemes for Idai (2019). They concluded all schemes failed to simulate the movement of Idai into Zimbabwe properly, showing the potential impact of shortcomings on the forcing model GFS. Our model simulations may have been subject to the same deficiency for hurricanes in general. They found the use of scale-aware schemes allows the model to resolve most of the dynamics. The wrong timing of the peak shows a need to use better performing global models as input for downscaling studies and operations.

5.2. Crop Simulations

In our study, the WOFOST simulations assumed the absence of pests and diseases. Pests and diseases lead to an estimated maize yield loss of about 22.5% or range of (19.5–41.1%) (Savary et al., 2019). Hence, our study focuses on relatively ideal scenario compared to reality. However, pests and diseases are not accounted for in the numerical treatment of vegetation and latent heat flux in the CFSv2 and WRF models. Therefore our experiments perform a fair evaluation of these models, and our experiments offer a good indication on the potential relative added value of downscaling the global seasonal forecasts. However, in reality the effects of pests and diseases may feedback to the atmospheric boundary layer as well through reduced evapotranspiration, adjusted surface energy partitioning and boundary-layer growth and entrainment. Unravelling these feedbacks is open for future study.

The WOFOST model has been configured for a water-limited production in which only the humidity parameters and water stress were factored (de Wit et al., 2019). Effective temperature plays a key role in the development stages of a crop while irradiation regulates CO_2 assimilation and partitioning (de Wit et al., 2019). For our simulation, all weather parameters were extracted from CFSv2 or WRF and a default CO_2 was assumed for our simulation. The assumption of a constant CO_2 is not completely realistic since it changes with seasons, but will not

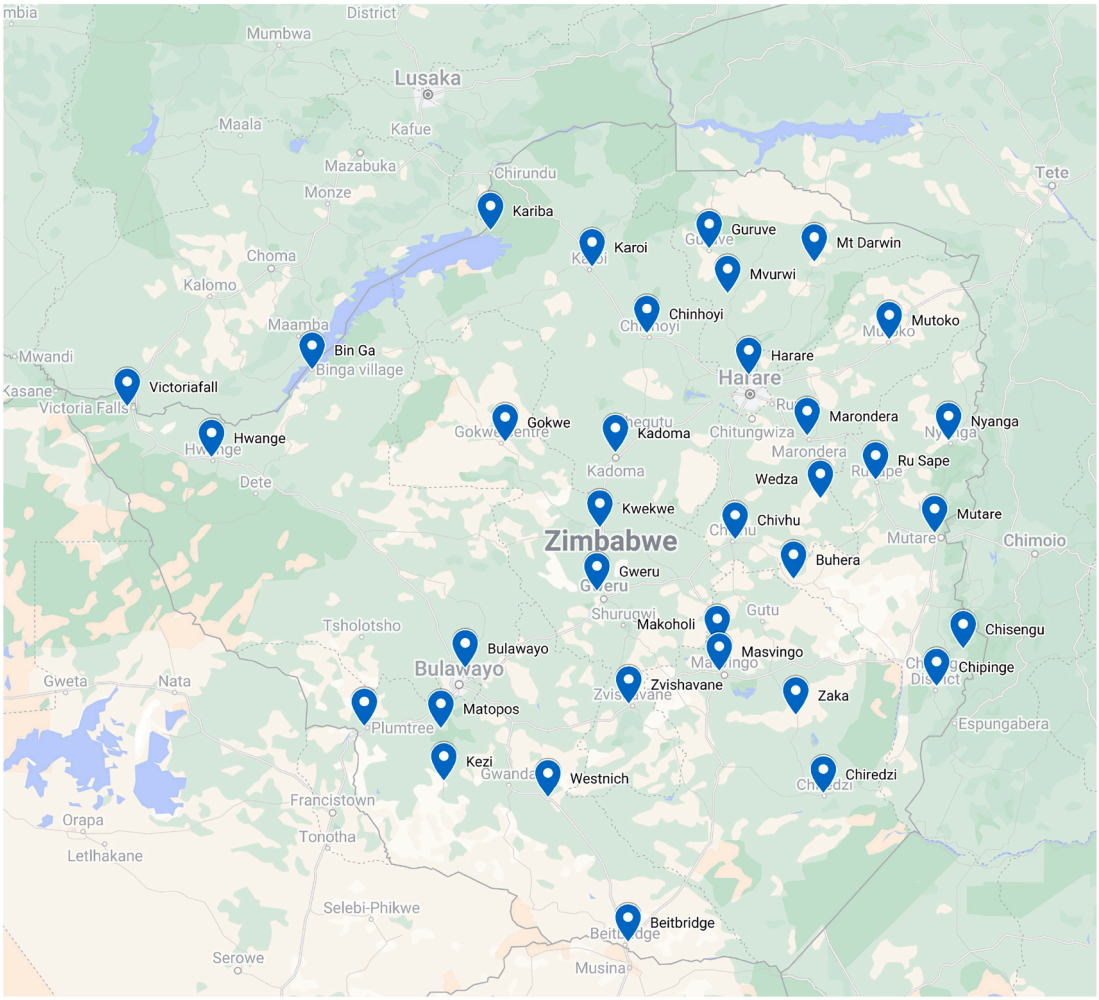

Fig. 8. Overview of weather station locations over Zimbabwe as used in this study.

affect the conclusions regarding the added value of downscaling. Finally, the evaluation of crop model was hampered by lack of actual yield values, especially on local and regional scales. Country-scale yield values are available, but did not offer meaningful observations. Therefore we recommend the setup and maintenance of more local and regional yield statistics.

6. Conclusions

This study evaluates the downscaling of CFSv2 deterministic seasonal forecasts (7 month lead time) over Zimbabwe for ten growing seasons (2011–2021) using the WRF mesoscale model. We pay special attention to the forecasted total seasonal rainfall in the different parts of the growing season. Subsequently we study the implications of the downscaling for WOFOST (water-limited) maize yield prediction for four regions (Karoi, Gweru, Masvingo, Beitbridge) in Zimbabwe.

We find that dynamical downscaling with WRF substantially improves the total seasonal rainfall estimates from CFSv2 in the growing season. Typically, CFSv2 total seasonal rainfall forecasts showed significant differences (Mann–Whitney-U test) with observed total seasonal rainfall for a large part of Zimbabwe compared to insignificant differences between WRF seasonal forecasts in October-December. Also for January-March and October-March, the differences between forecast and observations were higher for CFSv2 for almost the whole country compared to downscaled seasonal forecasts. These findings are reinforced from the scores for the standardised precipitation index (SPI) and the drought class. Moreover the anomaly correlation increased for the southernmost regions, but remained the same for the northern region. This indicates that the improved scores in the north are dominated by a better climatology while for the southern areas also the year to year variability improved due to downscaling.

Maize (*Zea mays L.*) yield forecasts (WOFOST) driven by downscaled WRF seasonal forecasts outperform their counterpart driven by CFSv2 with a MAPE reduction 8.3%-point (27% relative reduction) at Karoi. Considering the accumulated absolute yield error through the season, the WRF-forced maize yields performed better than CFSv2-forced simulations for more than half of the seasons for all sites (Fig. 7). The anomaly correlation for maize yield improved substantially for Gweru, Masvingo and Beitbridge, but remained the same for Karoi. So for the latter downscaling results in a better climatology while for the other sites the year to year varaiabily in crop yield was better captured. Overall we conclude that downscaled deterministic seasonal forecasts are beneficial for crop yield forecasts and as such for food distribution policies in Zimbabwe.

CRediT authorship contribution statement

S. Chinyoka: Conceptualization, Methodology, Software, Formal analysis, Visualization, Writing - original draft. **G.J. Steeneveld:** Conceptualization, Supervision, Writing - review & editing.

Declaration of Competing Interest

The authors declare that they have no known competing financial interests or personal relationships that could have appeared to influence the work reported in this paper.

Data availability

Data will be made available on request.

Acknowledgements

We thank Reinder Ronda (WUR) and Allard de Wit (WENR) for their advices, and the Meteorological Services Department of Zimbabwe for sharing rainfall observations. We acknowledge funding from NWO for SURFSARA supercomputing facilities (grant SH-312–15). We thank Imme Benedict (WUR) for her feedback on an earlier version of the manuscript.

Appendix A

Below we present an overview of the locations of the 35 weather stations used in this study.

References

Bae, S.Y., Hong, S.Y., Tao, W.K., 2019. Development of a Single-Moment Cloud Microphysics Scheme with Prognostic Hail for the Weather Research and Forecasting (WRF) Model, Asia-Pacific. J. Atmospheric Sci. 55, 233–245. https://doi.org/10.1007/s13143-018-0066-3.

Beilfuss, R., 2012. A risky climate for southern African hydro: assessing hydrological risks and consequences for Zambezi river basin dams, International Rivers 2150 Allston Way, Suite 300 Berkeley, CA 94704, USA, 2012. 10.13140/RG.2.2.30193.48486.

Bhatasara, S., 2017. Rethinking climate change research in Zimbabwe. J. Environ. Stud. Sci. 7, 39–52. https://doi.org/10.1007/s13412-015-0298-9.

Bopape, M.-J.M., Cardoso, H., Plant, R.S., Phaduli, E., Chikoore, H., Ndarana, T., Khalau, L., Rakate, E., 2021. Sensitivity of tropical cyclone idai simulations to cumulus parametrization schemes. Atmosphere 12. https://doi.org/10.3390/atmos12080932.

Chemura, A., Nangombe, S.S., Gleixner, S., Chinyoka, S., Gornott, C., 2022. Changes in climate extremes and their effect on maize (Zea mays L.) suitability over southern africa. Front. Climate 4. https://doi.org/10.3389/fclim.2022.890210.

Crétat, J., Pohl, B., Richard, Y., Drobinski, P., 2012. Uncertainties in simulating regional climate of southern africa: sensitivity to physical parameterizations using WRF. Clim. Dyn. 38, 613–634. https://doi.org/10.1007/s00382-011-1055-8.

de Lange, A., Naidoo, M., Garland, R.M., Dyson, L.L., 2021. Sensitivity of meteorological variables on planetary boundary layer parameterization schemes in the WRF-ARW model. Atmos. Res. 247, 105214 https://doi.org/10.1016/j.atmosres.2020.105214.

de Wit, A., Boogaard, H., Fumagalli, D., Janssen, S., Knapen, R., van Kraalingen, D., Supit, I., van der Wijngaart, R., van Diepen, K., 2019. 25 years of the wofost cropping systems model. Agric. Syst. 168, 154–167. https://doi.org/10.1016/j.agsy.2018.06.018.

Ebhuoma, E.E., 2022. Factors undermining the use of seasonal climate forecasts among farmers in south africa and zimbabwe: Implications for the 1st and 2nd sustainable development goals. Front. Sustainable Food Syst. 6 https://doi.org/10.3389/fsufs.2022.761195.

Favre, A., Hewitson, B., Lennard, C., Cerezo-Mota, R., Tadross, M., 2013. Cut-off Lows in the South Africa region and their contribution to precipitation. Clim. Dyn. 41, 2331–2351. https://doi.org/10.1007/s00382-012-1579-6.

Funk, C., Peterson, P., Landsfeld, M., Pedreros, D., Verdin, J., Shukla, S., Husak, G., Rowland, J., Harrison, L., Hoell, A., Michaelsen, J., 2015. The climate hazards infrared precipitation with stations - A new environmental record for monitoring extremes. Sci. Data 2, 1–21. https://doi.org/10.1038/sdata.2015.66.

Gilliam, R., Pleim, J., Xiu, A., 2007: Implementation of the pleim-xiu land-surface model and version 2 of the asymmetric, in: PBL model in the Weather Research and Forecasting Model (WRF). 8th WRF Users' Workshop, 2007, p. 5.7.

Guido, Z., Zimmer, A., Lopus, S., Hannah, C., Gower, D., Waldman, K., Krell, N., Sheffield, J., Caylor, K., Evans, T., 2020. Farmer forecasts: Impacts of seasonal rainfall expectations on agricultural decision-making in sub-Saharan Africa. Climate Risk Manage. 30, 100247 https://doi.org/10.1016/j.crm.2020.100247.

Hersbach, H., Bell, B., Berrisford, P., Hirahara, S., Horányi, A., Muñoz-Sabater, J., Nicolas, J., Peubey, C., Radu, R., Schepers, D., Simmons, A., Soci, C., Abdalla, S., Abellan, X., Balsamo, G., Bechtold, P., Biavati, G., Bidlot, J., Bonavita, M., De Chiara, G., Dahlgren, P., Dee, D., Diamantakis, M., Dragani, R., Flemming, J., Forbes, R., Fuentes, M., Geer, A., Haimberger, L., Healy, S., Hogan, R.J., Hólm, E., Janisková, M., Keeley, S., Laloyaux, P., Lopez, P., Lupu, C., Radnoti, G., de Rosnay, P., Rozum, I., Vamborg, F., Villaume, S., Thépaut, J.-N., 2020. The era5 global reanalysis. Quarterly J. R. Meteorological Soc. 146, 1999–2049. https://doi.org/10.1002/qj.3803.

Hong, S.-Y., Lim, K.-S., Kim, J.-H., Lim, J.-O.J., Dudhia, J., 2006. Wrf single-moment 6-class microphysics scheme (WSM6). J. Korean Meteorological Soc. 42, 129–151.

Ismail, S.A., 1987. Long-Range Seasonal Rainfall Forecast for Zimbabwe and Its Relation with EI-Nino/ Southern Oscillation (ENSO). Theoret. Appl. Climatol. 102, 93–102.

Jones, P.W., 1999. First- and second-order conservative remapping schemes for grids in spherical coordinates. Mon. Weather Rev. 127, 2204–2210. https://doi.org/10.1175/1520-0493(1999)127<2204:FASOCR>2.0.CO;2.

Kain, J.S., Kain, J., 2004. The Kain - Fritsch convective parameterization: An update. J. Appl. Meteorol. 43, 170–181. https://doi.org/10.1175/1520-0450(2004)043<0170:TKCPAU>2.0.CO;2.

Kassie, B., Van Ittersum, M., Hengsdijk, H., Asseng, S., Wolf, J., Rötter, R., 2014. Climate-induced yield variability and yield gaps of maize (Zea mays L.) in the central rift valley of Ethiopia. Field Crops Res. 160, 41–53. https://doi.org/10.1016/j.fcr.2014.02.010.

Kassie, B.T., Asseng, S., Rotter, R.P., Hengsdijk, H., Ruane, A.C., Van Ittersum, M.K., 2015. Exploring climate change impacts and adaptation options for maize production in the central rift valley of Ethiopia using different climate change

scenarios and crop models. Climatic Change 129, 145–158. https://doi.org/10.1007/s10584-014-1322-x.
Kerandi, N.M., Laux, P., Arnault, J., Kunstmann, H., 2017. Performance of the WRF model to simulate the seasonal and interannual variability of hydrometeorological variables in East Africa: a case study for the Tana River basin in Kenya. Theoret. Appl. Climatol. 130, 401–418. https://doi.org/10.1007/s00704-016-1890-y.
Keyantash, J., 2014: Standardized precipitation index (spi), https://climatedataguide.ucar.edu/climate-data/standardized-precipitation-index-spi, 2014. Accessed October 22 2019.
Kipkogei, O., Mwanthi, A.M., Mwesigwa, J.B., Atheru, Z.K.K., Wanzala, M.A., Artan, G., 2017. Improved seasonal prediction of rainfall over east africa for application in agriculture: Statistical downscaling of CFSv2 and GFDL-FLOR. J. Appl. Meteorol. Climatol. 56, 3229–3243. https://doi.org/10.1175/JAMC-D-16-0365.1.
Koster, R.D., Mahanama, S.P., Yamada, T.J., Balsamo, G., Berg, A.A., Boisserie, M., Dirmeyer, P.A., Doblas-Reyes, F.J., Drewitt, G., Gordon, C.T., Guo, Z., Jeong, J.H., Lawrence, D.M., Lee, W.S., Li, Z., Luo, L., Malyshev, S., Merryfield, W.J., Seneviratne, S.I., Stanelle, T., Van Den Hurk, B.J., Vitart, F., Wood, E.F., 2010. Contribution of land surface initialization to subseasonal forecast skill: First results from a multi-model experiment. Geophys. Res. Lett. 37, 1–6. https://doi.org/10.1029/2009GL041677.
Lo, J.C.-F., Yang, Z.-L., Pielke Sr., R.A., 2008. Assessment of three dynamical climate downscaling methods using the weather research and forecasting (WRF) model. J. Geophys. Res.: Atmospheres 113. https://doi.org/10.1029/2007JD009216.
Makadho, J., 1996. Potential effects of climate change on corn production in Zimbabwe. Climate Res. 6, 147–151. https://doi.org/10.3354/cr006147.
Makarau, A., Jury, M.R., 1997. Predictability of Zimbabwe summer rainfall. Int. J. Climatol. 17, 1421–1432. https://doi.org/10.1002/(sici)1097-0088(19971115)17:13<1421::aid-joc202>3.3.co;2-q.
Mamombe, V., Kim, W.M., Choi, Y.S., 2017. Rainfall variability over Zimbabwe and its relation to large-scale atmosphere–ocean processes. Int. J. Climatol. 37, 963–971. https://doi.org/10.1002/joc.4752.
Manatsa, D., Matarira, C.H., Mukwada, G., 2011. Relative impacts of ENSO and Indian Ocean dipole/zonal mode on east SADC rainfall. Int. J. Climatol. 31, 558–577. https://doi.org/10.1002/joc.2086.
Manjowe, M., Darlington Mushore, T., Vimbai Gwenzi, J., Mutasa, C., Matandirotya, E., Mashonjowa, E., 2018. Circulation mechanisms responsible for wet or dry summers over Zimbabwe. AIMS Environ. Sci. 5, 154–172. https://doi.org/10.3934/environsci.2018.3.154.
Matsui, T., Zhang, S.Q., Lang, S.E., Tao, W.K., Ichoku, C., Peters-Lidard, C.D., 2018. Impact of radiation frequency, precipitation radiative forcing, and radiation column aggregation on convection-permitting West African monsoon simulations. Clim. Dyn. 55, 1–21. https://doi.org/10.1007/s00382-018-4187-2.
Mishra, A., Hansen, J.W., Dingkuhn, M., Baron, C., Traoré, S.B., Ndiaye, O., Ward, M.N., 2008. Sorghum yield prediction from seasonal rainfall forecasts in Burkina Faso. Agric. For. Meteorol. 148, 1798–1814. https://doi.org/10.1016/j.agrformet.2008.06.007.
Mushore, T., 2013. Uptake Of Seasonal Rainfall Forecasts In Zimbabwe. IOSR J. Environ. Sci., Toxicol. Food Technol. 5, 31–37. https://doi.org/10.9790/2402-0513137.
Nikulin, G., Asharaf, S., Magariño, M.E., Calmanti, S., Cardoso, R.M., Bhend, J., Fernández, J., Frías, M.D., Fröhlich, K., Früh, B., García, S.H., Manzanas, R., Gutiérrez, J.M., Hansson, U., Kolax, M., Liniger, M.A., Soares, P.M., Spirig, C., Tome, R., Wyser, K., 2018. Dynamical and statistical downscaling of a global seasonal hindcast in eastern Africa. Climate Services 9, 72–85. https://doi.org/10.1016/j.cliser.2017.11.003.
Odekunle, T., 2004. Rainfall and the length of the growing season in Nigeria. Int. J. Climatol. 24, 467–479. https://doi.org/10.1002/joc.1012.
Ogutu, G.E., Franssen, W.H., Supit, I., Omondi, P., Hutjes, R.W., 2018. Probabilistic maize yield prediction over east africa using dynamic ensemble seasonal climate forecasts. Agric. Forest Meteorol. 250–251 243–261. https://doi.org/10.1016/j.agrformet.2017.12.256 https://www.sciencedirect.com/science/article/pii/S0168192317306767.
Phillips, J.G., Cane, M.A., Rosenzweig, C., 1998. ENSO, seasonal rainfall patterns and simulated maize yield variability in Zimbabwe. Agric. For. Meteorol. 90, 39–50. https://doi.org/10.1016/S0168-1923(97)00095-6.
Pohl, B., Crétat, J., Camberlin, P., 2011. Testing WRF capability in simulating the atmospheric water cycle over Equatorial East Africa. Clim. Dyn. 37, 1357–1379. https://doi.org/10.1007/s00382-011-1024-2.
Powers, J.G., Klemp, J.B., Skamarock, W.C., Davis, C.A., Dudhia, J., Gill, D.O., Coen, J.L., Gochis, D.J., Ahmadov, R., Peckham, S.E., Grell, G.A., Michalakes, J., Trahan, S., Benjamin, S.G., Alexander, C.R., Dimego, G.J., Wang, W., Schwartz, C.S., Romine, G.S., Liu, Z., Snyder, C., Chen, F., Barlage, M.J., Yu, W., Duda, M.G., 2017. The weather research and forecasting model: Overview, system efforts, and future directions. Bull. Am. Meteorol. Soc. 98, 1717–1737. https://doi.org/10.1175/BAMS-D-15-00308.1.
Ratnam, J.V., Behera, S.K., Ratna, S.B., et al., 2013. Dynamical downscaling of austral summer climate forecasts over southern Africa using a regional coupled model. J. Clim. 26, 6015–6032. https://doi.org/10.1175/JCLI-D-12-00645.1.
Reason, C., Landman, W., Tennant, W., 2006. Seasonal to decadal prediction of southern african climate and its links with variability of the atlantic ocean. Bull. Am. Meteorol. Soc. 87, 941–956. https://doi.org/10.1175/BAMS-87-7-941.
Robertson, A.W., Qian, J.-H., Tippett, M.K., Moron, V., Lucero, A., 2012. Downscaling of seasonal rainfall over the Philippines: Dynamical versus statistical approaches. Monthly Weather Rev. 140, 1204–1218. https://doi.org/10.1175/MWR-D-11-00177.1 https://journals.ametsoc.org/view/journals/mwre/140/4/mwr-d-11-00177.1.xml.
Rötter, R., 1993. Simulation of the Biophysical Limitations to Maize Production Under Rainfed Conditions in Kenya: Evaluation and Application of the Model WOFOST. Universität Trier.
Saha, S., Moorthi, S., Wu, X., Wang, J., Nadiga, S., Tripp, P., Behringer, D., Hou, Y.-T., et al., 2014. The NCEP climate forecast system version 2. J. Clim. 27, 2185–2208. https://doi.org/10.1175/JCLI-D-12-00823.1.
Savary, S., Willocquet, L., Pethybridge, S.J., Esker, P., McRoberts, N., Nelson, A., 2019. The global burden of pathogens and pests on major food crops. Nature Ecol. Evol. 3, 430–439. https://doi.org/10.1038/s41559-018-0793-y.
Schulzweida, U., 2014. Cdo user's guide uwe schulzweida-mpi for meteorology.
Shukla, J., 1998. Predictability in the midst of chaos: A scientific basis for climate forecasting. Science 282, 728–731. https://doi.org/10.1126/science.282.5389.728.
Skamarock, W., Klemp, J., Dudhia, J., Gill, D., Zhiquan, L., Berner, J., Wang, W., Powers, J., Duda, M.G., Barker, D.M., Huang, X.-Y., 2019. A Description of the Advanced Research WRF Model Version 4 NCAR Technical Note. National Center for Atmospheric Research, p. 145. https://doi.org/10.5065/1dfh-6p97.
Somses, S., Bopape, M.-J.M., Ndarana, T., Fridlind, A., Matsui, T., Phaduli, E., Limbo, A., Maikhudumu, S., Maisha, R., Rakate, E., 2020. Convection parametrization and multi-nesting dependence of a heavy rainfall event over namibia with Weather, Research and forecasting (WRF) model. Climate 8. https://doi.org/10.3390/cli8100112.
Stanski, H.R., Wilson, L.J., Burrows, W.R., 1989. A survey of common Verification Methods in Meteorology, 358, WMO World Weather Watch Technical Report No.8, WMO/TD.
Tadross, M.A., Hewitson, B.C., Usman, M.T., 2005. The interannual variability of the onset of the maize growing season over south Africa and Zimbabwe. J. Clim. 18, 3356–3372. https://doi.org/10.1175/JCLI3423.1.
Unganai, L.S., Mason, S.J., 2002. Long-range predictability of Zimbabwe summer rainfall. Int. J. Climatol. 22, 1091–1103. https://doi.org/10.1002/joc.786.
Unganai, L.S., Troni, J., Manatsa, D., Mukarakate, D., 2013. Tailoring seasonal climate forecasts for climate risk management in rainfed farming systems of southeast Zimbabwe. Climate Dev. 5, 139–152. https://doi.org/10.1080/17565529.2013.801823.
van Diepen, C.A., Wolf, J., van Keulen, H., Rappoldt, C., 1989. WOFOST: a simulation model of crop production. Soil Use Manag. 5, 16–24. https://doi.org/10.1111/j.1475-2743.1989.tb00755.x.
van Ittersum, M.K., van Bussel, L.G.J., Wolf, J., Grassini, P., van Wart, J., Guilpart, N., Claessens, L., de Groot, H., Wiebe, K., Mason-D'Croz, D., Yang, H., Boogaard, H., van Oort, P.A.J., van Loon, M.P., Saito, K., Adimo, O., Adjei-Nsiah, S., Agali, A., Bala, A., Chikowo, R., Kaizzi, K., Kouressy, M., Makoi, J.H.J.R., Ouattara, K., Tesfaye, K., Cassman, K.G., 2016. Can sub-Saharan Africa feed itself? Proc. National Acad. Sci. 113, 14964–14969. https://doi.org/10.1073/pnas.1610359113.
Washington, R., Todd, M., 1999. Tropical-temperate links in southern African and Southwest Indian Ocean satellite-derived daily rainfall. Int. J. Climatol. 19, 1601–1616. https://doi.org/10.1002/(SICI)1097-0088(19991130)19:14<1601::AID-JOC407>3.0.CO;2-0.
WFP, Zimbabwe, https://www.wfp.org/countries/zimbabwe/, 2019. Accessed September 20 2019.
Wilks, D.S., 2006. Statistical methods in the atmospheric sciences, second edition, 2, DOI: 10.1002/met.16.
Willmott, C., 1982. Some comments on the evaluation of model performance. Bull. Am. Meteorol. Soc. 63, 1309–1313. https://doi.org/10.1175/1520-0477(1982)063<1309:SCOTEO>2.0.CO;2.
WMO, Standardized Precipitation Index User Guide WMO-No. 1090, WMO-No. 1090 21 (2012) 1333–1348. DOI: 10.1175/2007JCLI1348.1.
Worldbank, Agriculture, 2021. forestry, and fishing, value added (% of gdp) - . Zimbabwe . https://data.worldbank.org/indicator/NV.AGR.TOTL.ZS?locations=ZW.
Yuan, X., Liang, X.Z., Wood, E.F., 2012. WRF ensemble downscaling seasonal forecasts of China winter precipitation during 1982–2008. Clim. Dyn. 39, 2041–2058. https://doi.org/10.1007/s00382-011-1241-8.
Ziervogel, G., Bithell, M., Washington, R., Downing, T., 2005. Agent-based social simulation: a method for assessing the impact of seasonal climate forecast applications among smallholder farmers. Agric. Syst. 83, 1–26. https://doi.org/10.1016/j.agsy.2004.02.009.